High-resolution CFD simulation of a plasma torch in 3 dimensions

L Klinger†§, J B Vos‡ and K Appert†

† CRPP, Swiss Federal Institute of Technology, CH-1015 Lausanne, Switzerland
‡ CFS Engineering, PSE-B, EPFL, CH-1015 Lausanne, Switzerland

E-mail: laurent.klinger@alcan.com

Abstract. We present results of 3D stationary simulations of electric arcs in Argon cross-flows, as typically found in plasma torches. A first study is devoted to electric arcs in a simple cross-flow geometry. The arc behaviour under varying flow conditions is found to be consistent with experimental works. Eventually, results in the geometry of a plasma torch used for thermal spraying are presented. Other aspects, like the strategy to obtain a converged calculation, the discussion of boundary conditions used for stationary simulations in cross-flows and a pseudo-temporal evolution of a restrike phenomenon, are also discussed.

Submitted to: *J. Phys. D: Appl. Phys.*

PACS numbers: 52.75Hn, 02.60Cb

§ Present address: Alcan Technology & Management SA, Ancien Sierre 9, CH-3960 Sierre, Switzerland

1. Introduction

Electric arcs have been known, studied and used for many decades. However, theoretical models describing the physics of the arc are only available for the most simple cases. With the increase of available computer resources in the last 20 years, much research has been undertaken to improve modelling of electric arcs, with the ambitious goal to be able to simulate numerically a working device, like a plasma torch.

As stated by Mäcker about fifty years ago already, the difficulty does not quite lie in the description of the phenomena occuring in such devices, but rather in the ability to compute the outcome of their interplay. The history of published research in the field supports this statement. Proceeding from crude 1D models (based on the Ellenbaas-Heller equation) to more realistic 3D models, each dimensionality was also characterised by an increased range of phenomena being taken into account. Without aiming at completeness, that evolution is seen from a quick look at the literature. For instance, Scott *et al* [1] performed 2D computations of a plasma torch using the so-called "fictious anode" model. Various other 2D simulations published in the literature dealt with several additional aspects of a torch model (or rather of a transferred arc in conditions similar to that of a torch). Examples are the work of Lowke *et al* [2] (who looked at sheaths and electrodes), Chang *et al* [3] (influence of nozzle shape on jet properties), Bauchire *et al* [4] (turbulence), Menart *et al* [5] (radiation transport), Schlitz *et al* [6] (time evolution) or Haidar [7] (non-LTE model).

In the last few years, several results of 3D simulations appeared in the literature, mostly using rather simple models to describe the arc. The very first 3D calculations were made for transferred arcs: even if they are axially symmetric, simulations were performed for such systems by Kaddani *et al* [8] (who even considered time-dependant situations). By submitting the arc to an external magnetic field, a true 3D arc configuration was obtained, and Speckhofer and Schmidt [9] as well as Schlitz *et al* [6] reported simulations for those conditions. However, even if 3D in nature, the flow pattern in these cases is still essentially axisymmetric. This lacks the distinguishing feature of arcs in plasma torches (or electric switches), where the (imposed) flow is perpendicular to the arc column. That situation was studied purely theoretically in 1986 by Mäcker and Stäblein [10], while Kelkar and Heberlein [11] were the first to tackle this problem numerically for an academic geometry (a rectangular duct). Then Freton *et al* [12] proposed a comparison between 2D and 3D calculations, showing good agreement for axisymmetric arcs. Li and Chen [13, 14] then published the first simulations of a 3D plasma torch on a rather coarse mesh considering the important gradients found in such devices. Finally, and most recently, Gonzalez *et al* [15] published another 3D simulation of a plasma torch. The last papers, as well as the present one, show that the modelling of arcs in cross-flows is still basic, tackling the easiest and most fundamental aspects of 3D models: that of the interaction between an arc column and a transverse flow, in stationary conditions, without the more elaborate aspects that have been explored in 2D.

It should be mentioned that looking for steady solutions is not an obviously reasonable thing to do from the physical point of view, since most operating conditions of a plasma torch correspond to non-stationary cases. However, there exist some choices of operational parameters where the arc column is stable (and stably attached at one point on each electrode [16]). In the following, we will present some flow solutions obtained in test cases similar to those presented by Kelkar and Heberlein [11], and obtained in the real geometry of a Sulzer-Metco F4 gun. The code used here is an academic CFD code (instead of the commercial CFD code Fluent frequently used nowadays). While more complex than a commercial code to work with, it provides with more freedom to extend it to a particular situation.

2. The model

We consider electric arcs in Argon at atmospheric pressure, with currents comprised between a few tens and a few hundreds Amperes, with the primary goal of studying the interaction between the flow and the arc column that is characteristic of cross-flow situations.

Under the assumption that the flow can be considered at local thermodynamic equilibrium (LTE, an assumption that is certainly not valid everywhere [17, 18], but nevertheless quite reasonable to make [19] as long as we are not interested in a correct description of the plasma-wall interaction near the arc feet or the arc column fringes), a one-fluid hydrodynamic model is used to describe the flow. Since the time evolution of the magnetic field in such a system can be estimated to be much quicker than that of the fluid [8, 20], one obtains a quasi-stationary description of the electromagnetic part, resulting in the following model: the complete Navier-Stokes equations, to which Ohmic heating and Lorentz force are added, and a Poisson-like equation for the electrical potential. In conservative form, this system is written as:

$$\partial_t \vec{W} + \partial_k(\vec{f_k} - \vec{q_k}) - \vec{S} = 0, \tag{1}$$

for $k = 1, 2, 3$ in 3D and where $\vec{W} = (\rho, \rho\vec{v}, \rho E, \phi)^T$ is the state vector containing the fluid variables density ρ, velocity $\vec{v}$ and total specific energy E, and the electric potential ϕ. The vectors $\vec{f_k}$ and $\vec{q_k}$ are the k-th component of the convective and dissipative flux density, respectively. They are written:

$$\vec{f_k} = \begin{pmatrix} \rho v_k \\ (\rho v_k)\vec{v} + p\vec{e_k} \\ (\rho E)v_k + pv_k \\ 0 \end{pmatrix}, \qquad \vec{q_k} = \begin{pmatrix} 0 \\ -\vec{\tau}\cdot\vec{e_k} \\ (\vec{\tau}\cdot\vec{v})_k + \kappa\,\partial_k T \\ \sigma\,\partial_k\phi \end{pmatrix}, \tag{2}$$

in which $\{\vec{e_k}\}_{k=1,2,3}$ is the canonical basis of $\mathbb{R}^3$, p is the pressure, T the temperature, $\vec{\tau}$ the stress tensor, κ the thermal conductivity and σ the electric conductivity. Finally, the source term $\vec{S}$ in (1) is written:

$$\vec{S} = (0, \vec{j}\wedge\vec{B}, \vec{j}^2/\sigma - U, 0)^T, \tag{3}$$

where $\vec{j} = -\sigma\nabla\phi$ is the electric current density, $\vec{B}$ the magnetic induction field and U a radiation term, respectively.

The system in (1) is closed by adding a state equation relating p and T to the chosen thermodynamic unknowns, ρ and E. Of course, for the high temperatures expected in plasma torches, where, in general, particle numbers as well as specific energies vary due to dissociation and ionization, the ideal gas law is not valid, and it must be replaced by a real gas relation, obtained using tabulated values of the thermodynamic properties of the gas under consideration [21]. In addition, tabulated values (for LTE conditions) are used for the transport coefficients, σ, κ, and μ, the viscosity (hidden in $\vec{\tau}$ in the above equations). The radiation is treated through a volumetric net emission coefficient U that depends on the gas state and is obtained from data published by Cram [22]. Let us remark that the above choice of the thermodynamic variables, a common choice in compressible CFD, leads to some technical difficulties with the thermodynamic and transport properties, which in general are given as function of pressure and temperature.

2.1. Boundary conditions

To solve the system (1), one must provide suitable boundary conditions. At the torch inlet, the temperature and velocity are given, as to obtain the desired mass flow of Argon. The pressure is imposed at the exit. On both inlet and outlet, the electrical potential is set to zero. Typically, the pressure was about 1 atmosphere, with an outlet pressure slighly lower; the temperature was either 300 K or 1000 K at inlet, depending on the case considered. On the electrodes, a zero velocity is imposed (no-slip condition). Then, either a temperature distribution or a zero heat flux is imposed. For the electric potential, the current density profile is typically given on the cathode (so as to obtain the total current at which the torch is operated), while the electric potential is set to zero on the anode.

These boundary conditions may be considered as 'standard' since they do not significantly differ from the ones usually given in the literature for arc simulations. However, in section 3.2 we shall discuss these boundary conditions for stationary calculations of arcs in cross-flows, as well as another choice of conditions that was eventually adopted to increase the numerical stability of the calculation.

2.2. The numerical method

The numerical method used to solve system (1) is briefly presented hereafter. This topic should not be considered as merely technical and straightforward, since the physics involved in the description of the system is highly non-linear (especially through the dependance of the electric conductivity on the temperature) and, consequently, means that obtaining a converged solution is non-trivial.

In order to solve the partial differential equations of the physical model by numerical means, a system of equations is built by approximating the differential operators in equations (1) at various points in the computational domain, which was meshed with a

structured mesh of hexaedra. The system is obtained by first applying a finite volume discretization to the spatial part of the model's equations. Then, the temporal part of the equations is discretised in an implicit way [23]. More formally, (1) is integrated on each volume Ω_i in the mesh, and assuming that $\vec{W}$ is constant throughout the volume, one obtains:

$$\frac{\mathrm{d}}{\mathrm{d}t}\left(V_i\,\vec{W}_i\right) + \vec{R}_i(\vec{W}_i) = 0, \tag{4}$$

where $\vec{R}_i$ is the residual in cell i (with volume V_i), which is the sum of the source term and of the net flux. The latter is the sum of the fluxes through each side of the cell. The temporal operator is then discretized:

$$V_i\frac{\vec{W}_i^{n+1} - \vec{W}_i^{n}}{\Delta t} + \theta\,\vec{R}_i(\vec{W}^{n+1}) + (1-\theta)\,\vec{R}_i(\vec{W}^{n}) = 0, \tag{5}$$

where the superscript n indicates the time level and θ is the *impliciteness*: when $\theta = 0$, the scheme is fully explicit, while it is fully implicit when $\theta = 1$. To solve 5, the residual at 'time' $n+1$ is linearized :

$$\vec{R}^{n+1} = \vec{R}^{n} + \frac{\partial \vec{R}}{\partial \vec{W}}\Delta\vec{W} + \mathcal{O}(\Delta t^2), \tag{6}$$

with $\Delta\vec{W} = \vec{W}^{n+1} - \vec{W}^{n}$. Eventually, the system of equations to solve is written

$$\left(\frac{V}{\Delta t}\mathbb{1} + \theta\frac{\partial \vec{R}}{\partial \vec{W}}\right)\Delta\vec{W} = -\vec{R}(\vec{W}^{n}). \tag{7}$$

(In the last equations, the subscripts i were dropped to indicate that all vectors subscripted with i are assembled in a single vector).

Even though we are only looking for a stationary solution, the temporal operators are kept, and used to drive the residual to zero, which is known as obtaining a *time-inaccurate* solution [24]. This procedure thus resembles a time evolution in which the various time steps are not known, but nevertheless retain their chronological order.

To solve (7), one must first provide approximations of the fluxes at the cell sides to build the right-hand side, then build the matrix corresponding to the operator notation $\partial\vec{R}/\partial\vec{W}$ (which amounts to linearize the fluxes with respect to the unknowns) and eventually solve the resulting system of equations. More specifically, the dissipative fluxes are discretized using a central formula, while the AUSM [25] scheme is applied to the convective fluxes. The resulting system is solved iteratively using a modified Gauss-Seidel scheme, with oblique sweeping, applied to an approximate lower/upper triangular decomposition of the matrix resulting from the discretisation.

The above method has been implemented in the CFD code NSMB [26] that was subsequently extended to take electric phenomena into account. NSMB natively considers viscous and compressible effects, even if the flow inside the torch can be considered as incompressible (but this may easily become inadequate outside the torch). The fact that NSMB does not use the same algorithm as in many other works in the field, which often rely on the SIMPLE family of computational methods due to Patankar

[27], provides a valuable consistency test between different methods that should yield comparable results.

Moreover, NSMB was written for use on parallel computers, which are needed to reach the high spatial resolution required by the strong gradients found in arc simulations. For the torch computations presented hereafter, the mesh contained about half a million cells.

2.3. Performing simulations

From the numerical point of view, obtaining a converged solution of a system of equations exhibiting very strong non-linearities is not trivial, and a variety of tricks are used in order to obtain an acceptable result. Therefore, it seems useful to describe here the main 'recipes' that were considered. It is appropriate to talk about these recipes in the frame of a physics paper because they are based on physical rather than on mathematical understanding.

In a first step, the simulations are performed with the fluid and electric parts decoupled. This allows to establish quickly a flow and a current channel between the electrodes. At this point, a channel of artificial electric conductivity, with peak value σ_c along a straight line connecting the two arc feet centres, is added to the natural electric conductivity and progressively removed during subsequent iterations. This approach is not merely a numerical convenience: one must find a way to obtain the effect of the electrical breakdown phenomena, whose physics is completely different from that of the established arc, and is not part of the model used. Note that in the real device, a high voltage RF pulse is used to initiate the breakdown.

Once the flow and the electric current are established, the electric and fluid parts are *slowly* coupled through a varying coefficient α multiplying the Ohmic term, j^2/σ, in (3). This coefficient can be calculated so that a specified and gradually increasing heating power is effectively dissipated in the flow (by summing the actual $(j_i^2/\sigma_i)V_i$ throughout all the cells i in the computational domain and computing the α that will 'normalize' that sum to the specified heating power). Starting with an effective Ohmic power as low as a few tens of Watts, it may reach tens of thousands of Watts, depending on the case being considered. Of course, the Ohmic power physically dissipated by the arc is not known beforehand, but it is possible to increase the effective Ohmic power up to a value estimated to be near the physical steady state value, for which the corresponding α should be also near 1. From this point, α is brought to 1 regardless of the associated effective Ohmic power, which comes as a result of the calculation, instead of a parameter to control the early iterations. However, it was observed that even if α is still an order of magnitude lower than 1, the flow may be quite near to its stationary state. In that situation, the final increase of α towards the value of 1 is reflected in a corresponding voltage drop, the power remaining roughly constant. As a consequence, since the flow configuration is close to the one it will assume in the stationary state, α can be then brought to 1 more quickly than during its former evolution. After that, iterations are

carried on until a satisfactory convergence level is attained.

Along with the use of α, various small interventions are made while $\alpha < 1$, such as, for example, filtering the electric potential, which may occasionally exhibit spurious oscillations in regions of large gradients where cells in the torch mesh have a high aspect ratio. Various other strategies were tried (such as performing subiterations on the electric potential during the strongest heating phases, so as to enforce current conservation at each iteration), but were far less effective. While resorting to tricks like filtering may appear to have no physical basis, it must be emphasised that any such help can be used during the iterations to drive the solution to a stationary state, as long as it is not effective any more in that state. When looking for steady states using an iterative procedure, it is not required that every iteration represents a physical state of the system.

It should be remarked that it is difficult to derive a convergence criterion valid for every case. For instance, when one performs a simulation with a low inlet velocity, one observes that the various diagnostics are (to a certain extent) quickly settling to fixed values (which are characteristic of the converged solution). But when the velocity is increased, some diagnosed quantities do not settle to an acceptable stationary state until, with sufficiently high inflow velocity, the computation diverges altogether as the arc is blown off by the cross-flow, an indeed physically perfectly acceptable answer of the numerical model.

3. Results

3.1. The rectangular duct

A simple case to consider that includes the most important features of arcs in cross-flows is one in a rectangular duct, whose geometry is sketched in figure 1 and which measures 5.2 by 2.2 by 2.2 cm. This configuration has been studied experimentally by Benenson and Cenkner [28] for low currents and velocities, and numerically for the same conditions by Kelkar and Heberlein [11]. The main feature of the arc behaviour observed experimentally is that, at fixed current, an increase of the cross-flow results in a hotter, narrower and more bent arc column. Conversely, at fixed inflow velocity, increasing the arc current results in a less bent and broader arc column.

Figure 2 displays a first result obtained for the same conditions as presented by Kelkar and Heberlein, which in turn was used to compare their results with the experimental measurements of Benenson and Cenkner. Both simulations are found to be in rather good agreement, the biggest difference being in the direction along the flow, where Kelkar and Heberlein obtain a steeper profile. However, in both cases, the radius of the column (defining it by the 8500 K isotherm) is the same. Figure 3 presents the evolution of the maximal temperature in a 60 A arc as function of the inlet velocity. For velocities above 1.4 m/s, the numerical solution exhibits unfading oscillations before breaking down above 2 m/s. For the same conditions, Benenson and Cenkner report

an "oscillatory mode" above 1.3 m/s (and, surprisingly, below 0.4 m/s; with our model, when trying to run at such low velocities, the iteration diverged).

The behaviour of the arc when either inflow velocity or arc current are increased is shown in figures 4 and 5. Figure 4 shows temperature profiles of a 100 A arc when the inlet velocity is increased from 2 to 10 m/s. As expected, the arc column is moving downstream with increasing velocity. For high velocities, the hottest point in the arc column is near the electrodes (thus, not in the figures plane, which is an yz plane at equal distance from the two electrodes, see figure 1) rather than in the centre of the arc. However, the downstream conditions are more strongly influenced by the increase of power dissipated by the arc than the arc core itself, since the most dramatic consequence of the velocity increase is seen downstream of the arc column.

Conversely, one may keep the inlet velocity at a fixed value and increase the current, and the result on the temperature and streamlines is shown in figure 5. Two effects of the current increase are clearly visible: the arc column moves upstream and assumes a more circular shape. This behaviour is consistent with the one observed by Benenson and Cenkner. However, the effect of the current variation on the streamlines seems almost insignificant when figure 5 is compared with figure 4. To explain this, it must be remembered that the streamlines shape "around" the hot core of the arc is due to the fact that the density in the arc is lowest in the centre, causing the cold and dense gas to flow around it. However, because the density goes roughly as the inverse of the temperature, even if the arc is hotter at higher current, it will not have a very different density profile, and thus, very different streamlines (for a fixed velocity).

3.2. More on boundary conditions

After the first simulations for the rectangular duct, it became clear that further research on boundary conditions was needed. It must be emphasised that performing stationary simulations implies that the arc feet should be fixed. However, with the 'standard' boundary conditions described in section 2.1, nothing hinders the anodic arc foot to move along with the cross-flow due to the absence of modelling of the electrodes themselves (they are not part of the computational domain, which is only made up of the flow) and of the non-equilibrium sheaths and ionization zones near the electrodes. Only a complete modelling of the actual electrodes (and the associated thermal inertia) would permit a stationary numerical solution without resorting to a special treatment of anode boundary. On the cathode side, things are less problematic since imposing the current profile effectively keeps the arc foot in place, but one may nevertheless question the choice of the current profile and its location. However, the relative independence of the results on the exact profile on the cathode [29] justifies the use of that condition.

To counter the effect of the cross-flow, one can think of several boundary conditions to keep the anodic arc foot in place. Kelkar and Heberlein used an anode of limited extent, followed downstream by a non-conducting wall where a zero normal current density is imposed, preventing the foot from moving beyond the extent of the anode.

The result is an extremely peaked current density profile at the downstream end of the anode. In our case, it prevented convergence in some high current cases, mainly due to the associated heating profile which would eventually cause the fluid part to diverge numerically.

Another solution would be to add an artificial electrical conductivity (with a smooth shape) near the arc foot to simulate a metallic tip permeable to the flow. That solution was found to be quite inefficient in keeping the arc foot in place. One could use more elaborate conditions that mix electric conductivity and/or temperature profiles (or zero heat flux) as well as the small anodic area *à la* Kelkar and Heberlein, but it was not always possible to remove the numerical instabilities at the downstream end of the anode.

Finally, it was possible to get rid of all problems associated with the need of fixing the anodic arc foot by also imposing a current profile at the anode. While this may seem much more artificial than the other possibilities enumerated above, it can be argued that the mere requirement of a fixed arc foot is itself utterly artificial (in absence of a complete thermal and electric modeling of the electrodes themselves).

3.3. The plasma torch

In this section, the numerical results of a plasma torch simulations are presented. The shape of the computational domain is shown in figure 6. It roughly corresponds to the F4 torch built by Sulzer-Metco. Three cases were considered: a 200 A arc at 30 SLPM (standard litres per minute) Argon and two 600 A arcs, one at 30 SLPM Argon and one at 50 SLPM. These conditions correspond to operating parameters allowing a stationary arc to establish (the so-called 'steady mode'). The temperature field obtained in the 200 A case is shown in figures 7 and 8. The first displays the temperature in the symmetry plane, which includes the arc feet. The second is drawn in a plane perpendicular to the symmetry plane, showing that the symmetry is effectively respected (in the non-helical injection considered). Note that the anode foot is arbitrarily chosen to be at the location where the path length to the cathode is the shortest, which seems physically sound.

For the 600 A case, it was possible to compare some numerical results with operational parameters of an F4 torch used at the CRPP. Experimentally, at 30 SLPM, an Ohmic power of 15.6 kW is obtained (corresponding to a tension of 26 V). Numerically, the numbers are 12.5 kW for the Ohmic power and 20.8 V for the voltage. The difference in voltage can be explained by the fact that the sheath and ionization zone are not part of the model, while it is known that the voltage drop is stronger there than in the arc column [30]. Let us remark that the 2D model (with fictious anode) of Scott *et al* [1], with comparable conditions, produced a 20 V tension, while their experiment showed a tension of 35 V. However, if the tension that was found in the present study makes sense, the energy balance is unsatisfactory. The various components of the energy balance are the following: 1.5 kW at the torch exit, 5 kW radiated, 4.9 kW as cooling

power, so that roughly 9 % of the energy produced is lost. The efficiency is then 12 %, about half what is measured.

Figure 9 shows the temperature and velocity profiles at the torch exit, along the symmetry plane. The local Mach number in the three cases shown reaches 0.13, 0.18 and 0.25 (ordered by increasing current and mass flow). This confirms the validity of the incompressibility assumption generally made for such simulations, but the highest value is not far from the value of 0.3 which is considered as the critical value above which compressibility effects should be taken into account. Note that the inflection at $z = -10^{-3}$ m in the velocity profiles is related to a purely numerical problem in the gradient evaluation on non-orthogonal meshes.

A better view of the flow in the torch can be seen in figure 10 which displays streamlines for the 600 A torch case. As expected, we see that most of the gas flows around (on both sides and below) the arc column. Also note that the arc column occupies roughly 65 % of a section perpendicular to the flow, while in the rectangular duct considered before the arc column is taking up about 80 % of the cross-section: as is felt intuitively, a rather small part of the incoming cold gas will actually approach the immediate vicinity of the arc column.

For the 600 A arc cases, the maximum temperature of about 30 000 K is obtained near the cathode foot, were the cross-flow is rather weak (compared to the anode arc foot, which is colder). Of course, in the absence of a more complete modelling of that part of the flow, one must not take too seriously the temperatures there, and in fact these are artificially limited by increasing the radiation above 29 000 K. This was done because the thermodynamic data used must be extrapolated above 30 000 K.

3.4. Towards temporal evolution

Although no time dependant simulations were performed, the stationary solutions were sought using a pseudo-temporal solution process which yielded interesting intermediate results.

Figure 11 shows a sequence of temperature cuts in time-like order for a 60 A arc with an inlet velocity for which no steady solution could be obtained (as is obvious from the figure). Although the calculation started with a straight arc column (because of an initially straight σ_c channel), as soon as the artificial electric conductivity channel is lowered, the arc is quickly bent by the flow, as is shown in the last sections. However, contrary to the runs presented in section 3.1, the straight channel of artificial electric conductivity was maintained at a low value, namely $\sigma_c = 50$ mho/m, which is negligible with respect to the typical values of the conductivity in the arc core, that are 100 times higher.

Starting from the iteration whose state is shown in the first picture of figure 11 (top left), it is seen that the arc continues to bend under the cross-flow. When it becomes sufficiently elongated, a small (but increasing) fraction of the current flows through the artificial electric conductivity channel (top right). Since σ_c is low there, even a small

current density is able to produce substantial heating. This results in a secondary arc column which is much shorter than the primary one. Subsequently, the secondary arc is heated up rapidly (in a number of iterations sense). In the end, that shorter column carries all the current and what was the primary arc dies. At this "time" it is the new arc's turn to be bent by the cross-flow, until it assumes the same state as depicted in the first picture and the process starts all over again.

Of course, this kind of behaviour will inevitably be considered in relation with a typical mode of operation of plasma torches called 'restrike'. The observation in the experiment is a quasi-periodic phenomenon characterised by a sawteeth-like behaviour of the voltage which gradually increases (apparently when the arc length grows) and then rapidly crashes (when the new, shorter arc becomes the relevant current channel, i.e. when it "restrikes").

It is clear that a simple hydrodynamic model assuming local thermodynamic equilibrium (like our's) is not appropriate to simulate such a phenomenon even if it were correctly time-dependent. In such a model, the electron density upstream outside the arc channel is exponentially small; in fact, it is zero for all practical purposes in the area where the restrike occurs. In reality the secondary arc channel must be born in a small non-equilibrium electron population maintained upstream by radiation from the arc column and root—or by some other hypothetical means. In the simulation presented above, the negligible σ_c left upstream can be seen as qualitatively playing the role of this electron population.

4. Discussion

The solutions obtained for the rectangular duct demonstrate that the simulations are at least able to reproduce the main features of the behaviour of the arc in a cross-flow, as expressed by the empirical laws of Benenson and Cenkner (cf. section 3.1). Looking at the various diagnostics implemented in the code, those results can be well understood. For instance, one sees that cooling the arc by increasing the cold cross-flow results in an arc that dissipates more power as it is stretched and bent, thus compensating the enhanced cooling and thus being able to maintain itself.

While results in the rectangular duct can be examined from several points of view (comparison with experimental and numerical works, internal physical consistency), and were found to be satisfactory in this respect, the case of the plasma torch is far less clear. Comparison with experimental studies is difficult, since the literature for corresponding conditions is sparse at best. At the very least, the model presented is able to obtain a converged stationary solution in the conditions of the so-called 'steady-mode' of the F4 torch operated with pure Argon (conditions described in section 3.3). The behaviour of the temperature and velocity at the torch exit is also consistent with experimental observations made at CRPP [31] when the current and inlet velocity are varied. Note, however, that they are not the same as in the rectangular duct, where a velocity increase at the inlet also causes a large change in the temperature at the exit, contrary to the

torch situation.

Concerning the numerical consistency, it must be pointed out that the energy balance of the torch solutions was less than satisfactory, since it turns out that approximately 9 % of the energy input (which is essentially due to Ohmic heating) is lost and not found in the energy output. Considering the results of the various cases in the torch geometry, it seems probable that fixing this problem will mainly result in slightly higher exit velocities (but not much higher exit temperatures). Even if the energy balance were correct, one must nevertheless emphasize the uncertainty that exists on the relative contributions of the different terms, since the radiation appears of paramount importance at high currents. There is little doubt that questions remain with this respect, considering the crude modelling of the radiation. However, it seems that a more elaborated model to account for radiation will require a considerable computing power that is not yet commonly available for 3D calculations.

Considering the results of the simulations presented here, it is appropriate to discuss the modelling status of plasma torches and possible future directions of research. It is clear, both from experiments and numerical simulations, that steady-state arc simulations in a cross-flow merely are a first step and that one should consider in the near future time-dependent conditions. This would certainly turn out to be far more interesting for the experimentalist as well as for the numerical scientist, since the physics is closer to actual 'real life' conditions. However, the move to time-dependent simulations requires the inclusion of the electrodes into the numerical model in order to treat the moving arc foot in a satisfactory way. Time-dependent simulations serve two objectives: (a) obtaining a stationary arc in the same typical conditions as above and (b) obtaining restrike frequencies. The first objective certainly serves as a test case, but it also answers the interesting question why an arc in a cross-flow would be stationary in the first place. In the results presented in this paper, the arc position was fixed, but this does not make sense in time-dependent situations. Meeting the second objective would mean an enormous step forward for arc simulations and make comparison with experiments easier.

5. Conclusion

A numerical model for 3D arcs at atmospheric pressure in a cross-flow has been presented. It assumes one-fluid hydrodynamic flows at local thermodynamic equilibrium. To solve the corresponding equations, a finite volumes discretization is used as well as a time-inaccurate iteration to obtain steady states. Two main configurations were considered: an arc in a rectangular duct and the F4 plasma torch. In the first case, the effect of the inlet velocity and arc current has been observed and found to be consistent with published experimental works. Moreover, boundary conditions to obtain stationary arcs in cross-flows are discussed and a sequence of unsteady states resembling the 'restrike mode' is shown.

Acknowledgments

We thank Jean-Luc Dorier and Laurent Sansonnens for the fruitful discussions about experimental and modelling aspects of plasma torches, as well as their comments on the manuscript. The thermodynamic data for Argon has been provided by Tony Murphy (CSIRO), to whom we are indebted. All the computations have been performed on the computers of the Service Informatique Central of the Swiss Federal Institute of Technology in Lausanne, in particular on the Origin 3000 and the Swiss T-1. This work was partially supported by the Swiss National Science Foundation.

References

[1] Scott D A, Kovitya P and Haddad G N 1989 *J. Appl. Phys.* **66** 5232
[2] Lowke J J, Morrow R and Haidar J 1997 *J. Phys. D: Appl. Phys.* **30** 2033
[3] Chang O H, Kaminska A and Dudeck M 1997 *Journal de physique III* **7**(4) 1361
[4] Bauchire J-M, Gonzalez J-J and Gleizes A 1997 *Journal de physique III* **7**(4) 829
[5] Menart J, Malik S and Lin L 2000 *J. Phys. D: Appl. Phys.* **33** 257
[6] Schlitz L Z, Garimella S V and Chan S H 1999 *J. Appl. Phys.* **85**(5) 2540
[7] Haidar J 1999 *J. Phys. D: Appl. Phys.* **32** 263
[8] Kaddani A, Zahrai S, Delalondre C and Simonin O 1995 *J. Phys. D: Appl. Phys.* **28** 2294
[9] Speckhofer G and Schmidt H-P 1996 *IEEE Transactions on Plasma Science* **24**(4) 1239
[10] Mäcker H H and Stäblein H G 1986 *IEEE Transactions on Plasma Science* **14**(4) 291
[11] Kelkar M and Heberlein J 2000 *J. Phys. D: Appl. Phys.* **33** 2172
[12] Freton P, Gonzalez J-J and Gleizes A 2000 *J. Phys. D: Appl. Phys.* **33** 2442
[13] Li H-P and Chen X 2001 *J. Phys. D: Appl. Phys.* **34** L99
[14] Li H-P and Chen X 2002 *Chinese Physics* **11** 44
[15] Gonzalez J-J, Freton P and Gleizes A 2002 *J. Phys. D: Appl. Phys.* **35** 3181
[16] Dorier J-L, Gindrat M, Hollenstein C, Salito A, Loch M and Barbezat G 2001 *IEEE Transactions on Plasma Science* **29** 494
[17] Bober L and Tanking R S 1970 *J. Quant. Spectrosc. Radiat. Transfer* **10** 991
[18] Gleizes A, Kafrouni H, Duc H D and Maury C 1982 *J. Phys. D: Appl. Phys.* **15** 1031
[19] Haidar J 1995 *J. Phys. D: Appl. Phys.* **28** 2494
[20] Klinger L 2002 *Simulation numérique 3D d'une torche à plasma par une méthode de volumes finis* (PhD thesis 2687, Swiss Federal Institute of Technology, Lausanne)
[21] Murphy A B 2001 *J. Phys. D: Appl. Phys.* **34** R151
[22] Cram L E 1985 *J. Phys. D: Appl. Phys.* **18** 401
[23] Weber C 1998 *Development of Implicit Methods for the Navier-Stokes Equations and Large Eddy Simulation: Application to External Aerodynamics* (PhD thesis, INPT Toulouse)
[24] Jameson A and Turkel E 1981 *Mathematics of Computation* **37**(156) 385
[25] Liou M-S, Christopher J and Steffen J 1993 *J. Comp. Phys.* **107** 23
[26] Vos J B, Rizzi A W, Corjon A, Chaput E and Soinne E 1998 *Recent Advances in Aerodynamics inside the NSMB Consortium* (Reno NV, 36th Aerospace Sciences Meeting & Exhibit)
[27] Patankar S V 1980 *Numerical Heat Transfer and Fluid Flow* (Washington: Hemisphere Publishing Corporation)
[28] Benenson D M and Cenkner A A 1970 *Journal of Heat Transfer* 276
[29] Wenelstorf J 2000 *Ab initio modelling of thermal plasma discharges (electric arcs)* (PhD thesis, TU Braunschweig)
[30] Pfender E 1978 *Electric Arcs and Arc Gas Heaters, in Gaseous Electronics, Vol I, Electric Discharges* (London: Academic Press)

[31] Dorier J-L, private communication

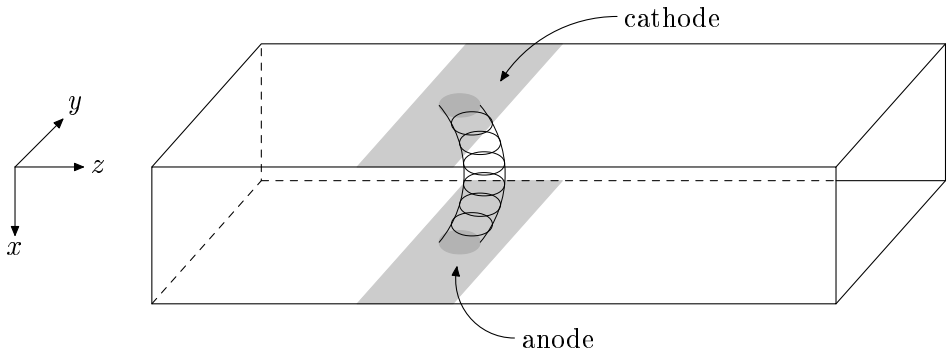

Figure 1. Sketch of an arc in a cross-flow. It is for that kind of arrangement that we compare in figure 2 our computational results with those obtained by Heberlein and Kelkar.

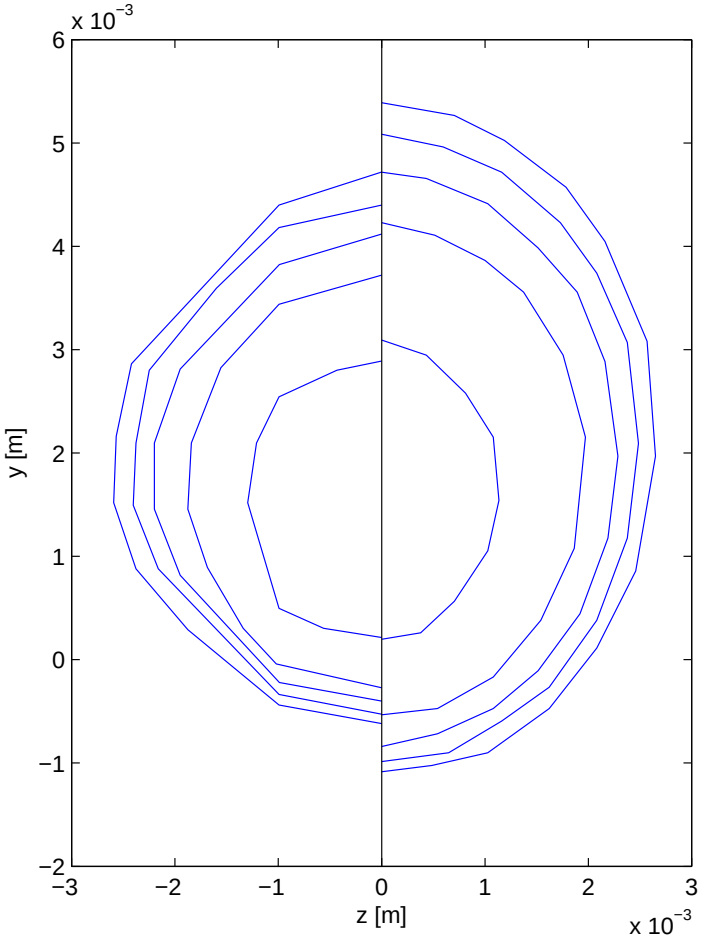

Figure 2. Isotherms in the mid-section of a 34 A arc in Argon, according to Kelkar and Heberlein (left) and our simulation (right). The isotherms are, from inside to outside, 10 200 K, 9500 K, 9100 K, 8800 K and 8500 K.

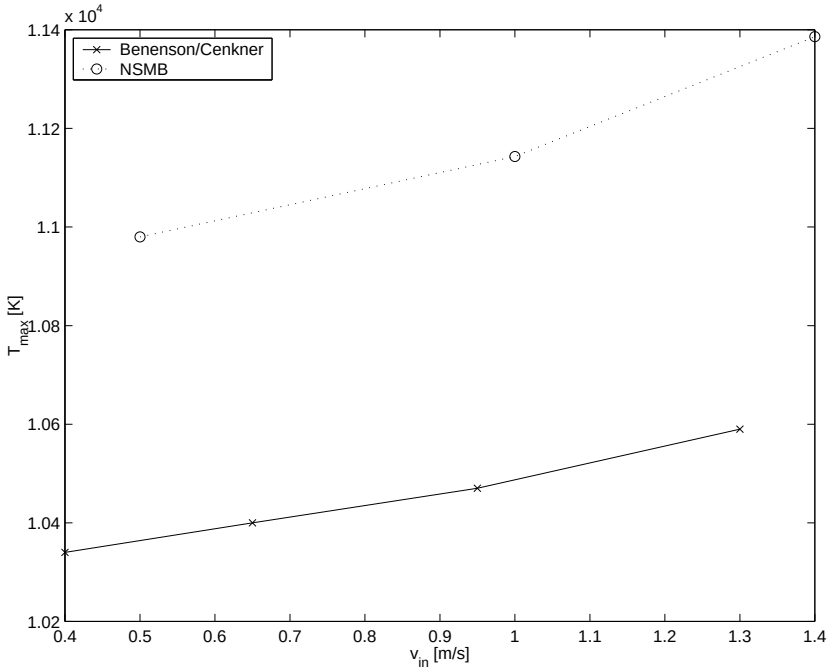

Figure 3. Maximal temperature in a 60.3 A arc as function of the inlet velocity, compared with the measurements of Benenson and Cenkner.

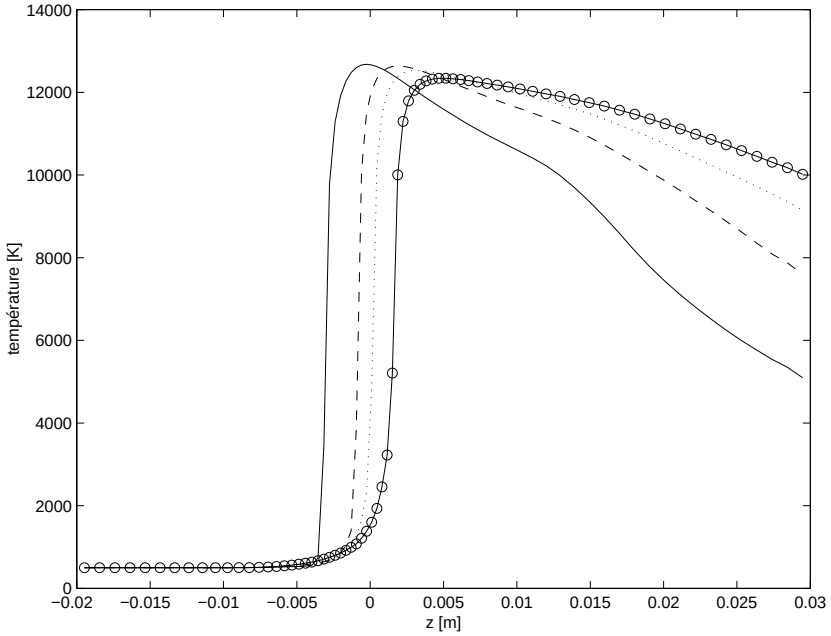

Figure 4. Temperature profiles for a 100 A arc in a cross-flow, for inlet velocities of 4 m/s (——), 6 m/s (– – –), 8 m/s (· · · · · ·) and 10 m/s (-o-). The profile line is in the symmetry plane of the arc, at an equal distance of both electrodes, the flow coming from the left.

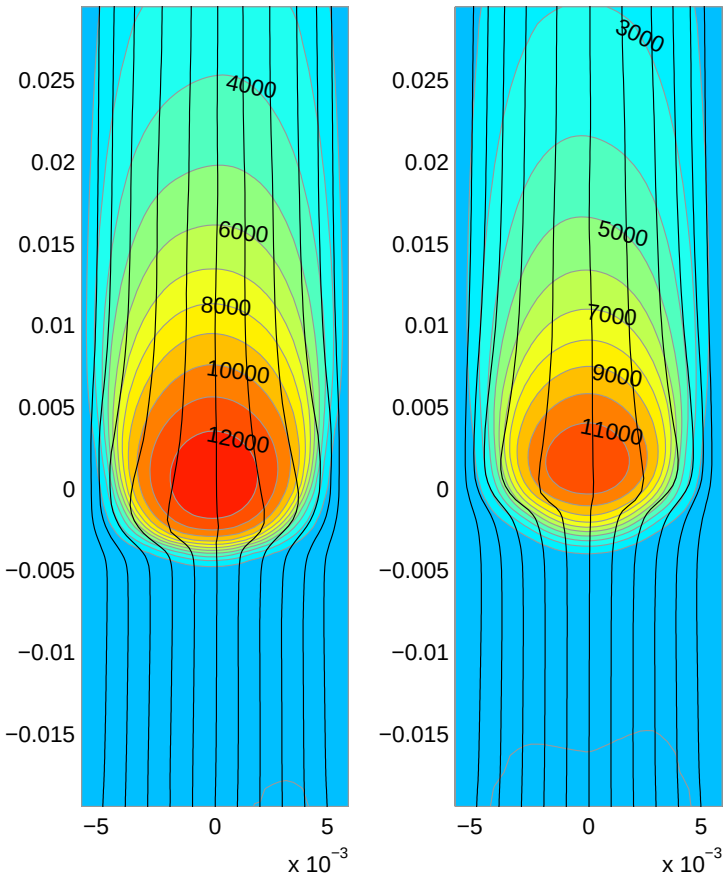

Figure 5. Isotherms and streamlines for a 60 A and a 120 A arc in a cross-flow, for a fixed inlet velocity of 1 m/s. The graph plane is in the symmetry plane of the arc, at an equal distance of both electrodes. The arc feet are at 0 on the vertical axis.

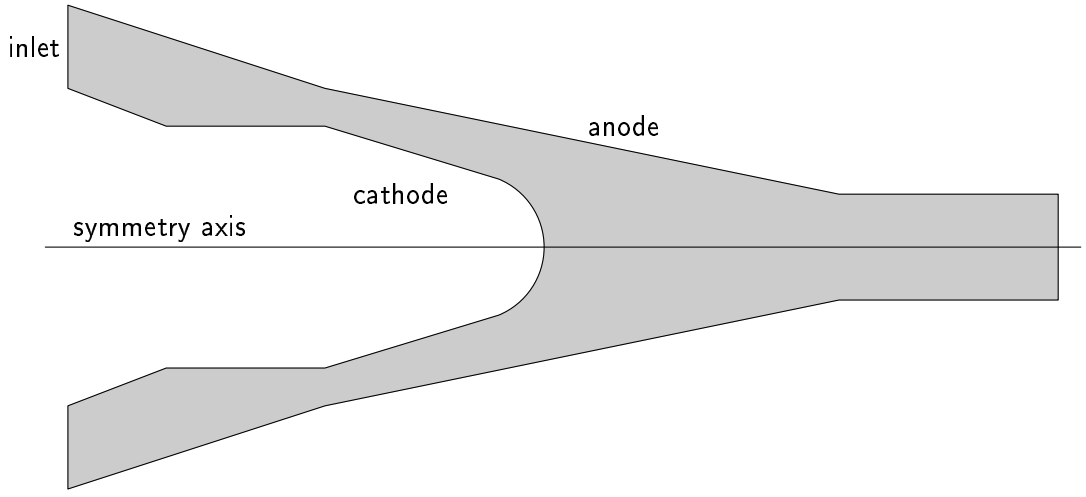

Figure 6. Schematic view of the torch geometry. The grey part is the computational domain, which extends on 5.2 cm.

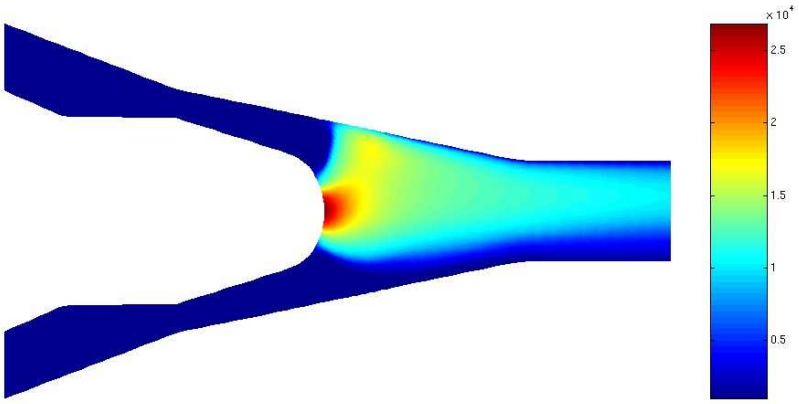

Figure 7. Temperature in the symmetry plane of a 200 A torch. In this figure, the cathode foot is at the tip of the cathode, while the anode foot is on the upper part of the anode, where the temperatures are higher.

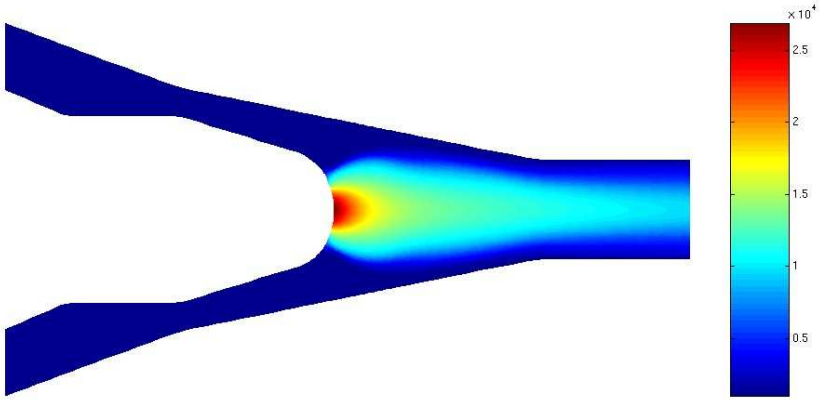

Figure 8. Temperature in the plane perpendicular to the symmetry plane of a 200 A torch.

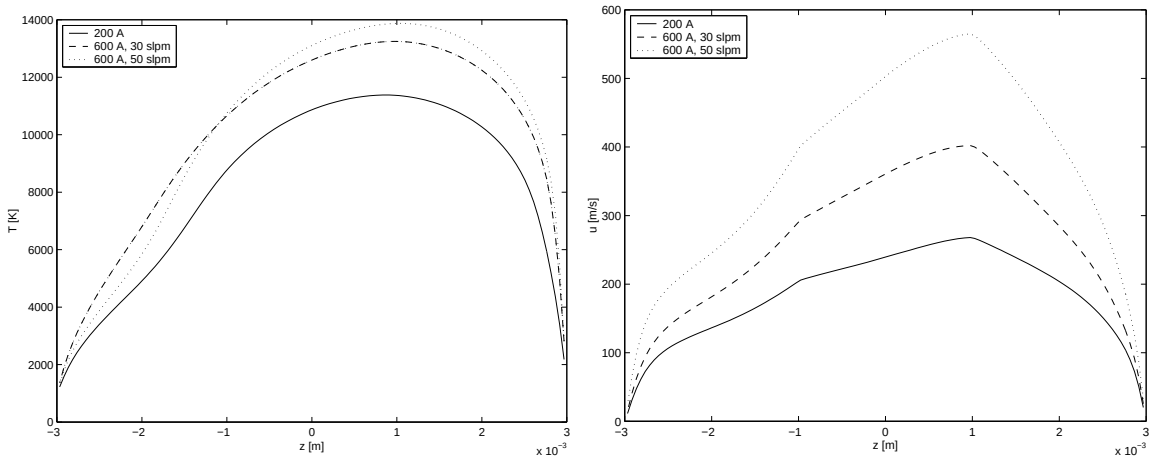

Figure 9. Temperature and velocity profiles at the torch exit, for 200 A and 600 A cases.

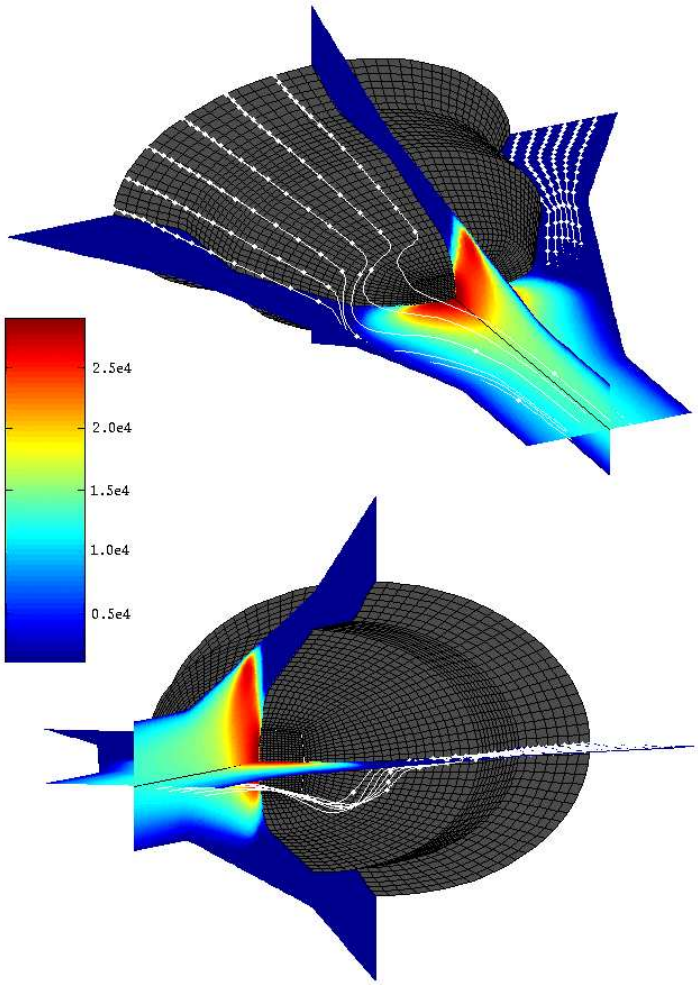

Figure 10. Temperature and streamlines in a 600 A torch, at 30 SLPM. The massless particles used to draw the streamlines are released in two groups, one along a quarter circle between the electrodes at inlet and the other on a radial line perpendicular to the symmetry plane also at inlet.

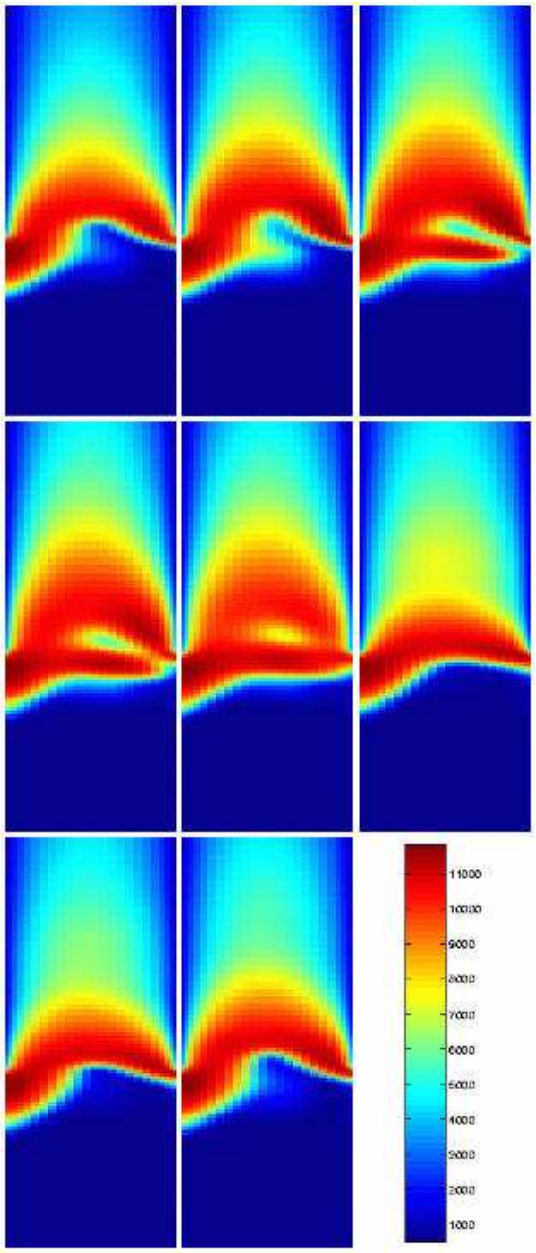

Figure 11. Pseudo-temporal evolution of the temperature for an arc in a cross-flow at high inlet velocity, when a negligible artificial electric conductivity channel is maintained.